Analytical and Bioanalytical Chemistry (2020) 412:5811–5817
https://doi.org/10.1007/s00216-020-02803-5

RESEARCH PAPER

Silanized carbon dot-based thermo-sensitive molecularly imprinted fluorescent sensor for bovine hemoglobin detection

Yajing Zhao[1] · Yujuan Chen[1] · Mengyao Fang[1] · Yabing Tian[1] · Guangyue Bai[1] · Kelei Zhuo[1]

Received: 24 May 2020 / Revised: 22 June 2020 / Accepted: 2 July 2020 / Published online: 11 July 2020

Abstract

Using the surface molecular imprinting technique, a thermo-sensitive molecularly imprinted fluorescent sensor was constructed for bovine hemoglobin (BHb) detection with the silanized carbon dots (CD@SiO_2) as fluorescent signal, N-isopropylacrylamide as monomer sensitive to temperature, and BHb as template. The silanized carbon dots coated by the molecularly imprinted polymer (CD@SiO_2@MIP) were characterized by high-resolution transmission electron microscopy, Fourier transform infrared spectroscopy, and fluorescence spectroscopy. Owing to the combination of the strong fluorescence sensitivity of CDs and the high selectivity of the molecular imprinting shell, the prepared sensor showed good recognition and detection performance to the target protein BHb, with a linear range of 0.31–1.55 μM and a detection limit of 1.55 μM. Furthermore, the sensor was utilized to detect the content of BHb in real urine with a recovery of 98.6–100.5%. The CD@SiO_2@MIP sensors present a high potential for applications in the detection of BHb in biological systems.

Keywords Molecularly imprinted polymer · Bovine hemoglobin · Carbon dot · Fluorescence sensor · Silanization

Introduction

Hemoglobin (Hb) is a major component of red blood cells. It binds to oxygen and transports oxygen and carbon dioxide, and plays a particularly important role in many physiological activities [1]. Its content is a good indicator of anemia. For example, it is low in symptoms such as anemia, palpitations, and lack of blood color [2]. Therefore, the research of Hb is greatly important for proteomics and clinical diagnosis. Since the similarity of bovine hemoglobin (BHb) with Hb reaches above 90% [2, 3], BHb is generally applied as an alternative for Hb.

Molecularly imprinted polymers (MIPs) have specific binding sites that are complementary to size, shape, and function-group position of the template molecule [4, 5]. Compared with other recognition systems, MIPs have unique structure predictability, recognition specificity, and application universality, and thus are widely used in molecular recognition and protein capture. At present, the development of imprinting of small molecules is relatively complete due to simple molecular structure and easy imprinting process. Scientists have successfully developed many MIPs of small molecules [6–10]. However, the imprinting of biological macromolecules such as proteins or viruses still faces significant challenges due to their large size, complex structure, and sensitivity to the environment [11–13].

Now, methods for preparing protein MIPs mainly include epitope imprinting [14, 15], surface imprinting [16, 17], and metal chelation imprinting [18, 19]. In the surface imprinting, the template molecules can be completely removed from the MIPs, and therefore, the MIPs can provide good accessibility to the target protein molecules, which largely solves the problems of low sensitivity and long response time of the sensor. Consequently, the surface imprinting has become one of commonly used methods for macromolecular imprinting. In addition, other fluorescence methods based on the innovative gated resonance energy transfer have recently been developed for the detection of proteins with high sensitivity [20, 21].

Meanwhile, the construction of fluorescence sensing systems is a feasible approach for sensitive detection of proteins

Electronic supplementary material The online version of this article (https://doi.org/10.1007/s00216-020-02803-5) contains supplementary material, which is available to authorized users.

✉ Kelei Zhuo
klzhuo@263.net

[1] Collaborative Innovation Center of Henan Province for Green Manufacturing of Fine Chemicals, Key Laboratory of Green Chemical Media and Reactions, Ministry of Education, School of Chemistry and Chemical Engineering, Henan Normal University, Xinxiang 453007, Henan, China

and other biological macromolecules. At present, some research groups have reported on molecularly imprinted fluorescent sensors for detecting BHb based on different fluorescent materials [12, 13]. Among these fluorescent materials, carbon dots (CDs), compared with conventional fluorescence materials like semiconductor quantum dots (QDs) and fluorescence dyes, have low toxicity, good biocompatibility, and excellent optical property, and thus have attracted much attentions in the field of chemical sensing [22–28]. Since CD-based molecularly imprinted fluorescence sensors combine the fluorescence sensitivity of CDs with the high selectivity of MIPs, they have stood out in many areas such as chemical and biological analyses [29]. For example, they have been utilized to detect trace analytes in complex samples. However, the CD-based molecularly imprinted fluorescent sensors also have disadvantages, such as easily affecting fluorescence intensity [26]. To solve this problem, we have used the silanization technique to protect the fluorescent intensity of silica-coated CD (CD@SiO_2) [30].

Here, we report a new thermo-sensitive molecularly imprinted fluorescence sensor (CD@SiO_2@MIP) for the detection of BHb. In the preparation process of CD@SiO_2@MIP, CDs were silanized, which play a role of fluorescence signal and carrier for deeply imprinting procedure. Thermo-sensitive property and fluorescent sensing performance of CD@SiO_2@MIP as probe to BHb were studied. Finally, the sensor was successfully used for BHb detection in real urine samples, indicating a powerful potential for detection of the target protein in biological systems.

Experimental section

Chemicals and materials

The chemicals and materials and instruments utilized are put in the Electronic Supplementary Material (ESM).

Preparation of CD@SiO_2@MIPs

Carbon dots with blue fluorescence were prepared by one-step hydrothermal method according to the literature [31]. The silica-coated CD (CD@SiO_2) were prepared with the Stöber method [32] with some modifications. The experimental details for preparing CD and CD@SiO_2 are given in the ESM. The CD@SiO_2 coated with MIP (CD@SiO_2@MIP) was synthesized using the surface imprinting method [33]. First of all, the CD@SiO_2 composite was dispersed into 10 mL phosphate buffer solution (PBS, pH = 6.8). Then, 80 mg of *N*-isopropylacrylamide (NIPAAm) as the thermo-sensitive monomer, 30 μL of methacrylic acid (MAA) as the functional monomer, 25 mg of the template BHb, and 20 mg of *N,N*-methylenebis(acrylamide) (MBA) as the cross-linking agent were added sequentially to the dispersion system under stirring at 25 °C for 4.5 h to pre-polymerize. Thirdly, the polymerization was initiated by adding 10 mg of ammonium persulfate (APS) as the initiator and 100 μL of *N,N,N′,N′*-tetramethylethylenediamine (TEMED) as the catalyst under nitrogen atmosphere, and the polymerization was carried out at 25 °C for 20 h. Finally, the product was centrifuged and washed repeatedly with the SDS (1 g) + acetic acid (10 mL) + DI-water (90 mL) solution until the template BHb molecules could not be detected by UV-vis spectrophotometry. Using the same method without addition of BHb template, we also prepared corresponding non-imprinted polymer material (CD@SiO_2@NIP) for comparison.

Binding experiments

The adsorption kinetic curves were measured and are presented in Fig. S3 (see ESM). Briefly, 80 mg of CD@SiO_2@MIP composite was dissolved into 10 mL of PBS (0.01 M, pH = 6.8). Then, 10 mL of BHb (1 mg/mL) solution was added to the CD@SiO_2@MIP dispersion and incubated for 1 h. After centrifugation at 10000 rpm for 15 min, the absorbance of supernatant was measured with a UV-vis spectrophotometer at 405.5 nm to determine concentration of BHb in the supernatant. The adsorption amount (Q, mg/g) was computed by

$$Q = (c_0 - c_r)V/m \quad (1)$$

where c_0 and c_r (mg/mL) are the original and the residual concentration of BHb, respectively, V (mL) is the solution volume, and m (g) is the mass of CD@SiO_2@MIP. For CD@SiO_2@NIP, similar method was used.

Fluorescence measurements

Fluorescent intensity detection was performed with a FLS-980 spectrofluorometer, with 6 nm of slit width for the excitation and emission, 345 nm of excitation wavelength, and a recording range of 365–600 nm of emission wavelength. After adding a given concentration of BHb solution in the dispersion of CD@SiO_2@MIP, the mixture was shaken for 60 min and then scanned.

Urine samples

The urine sample was filtered through a microfiltration membrane (0.22 μm) for removing particulate matter, and then was diluted 100-fold for use. The recovery was determined using the standard addition method with 0.5, 1.0, and 1.5 μmol/L of BHb. Each sample was parallelly measured at least three times.

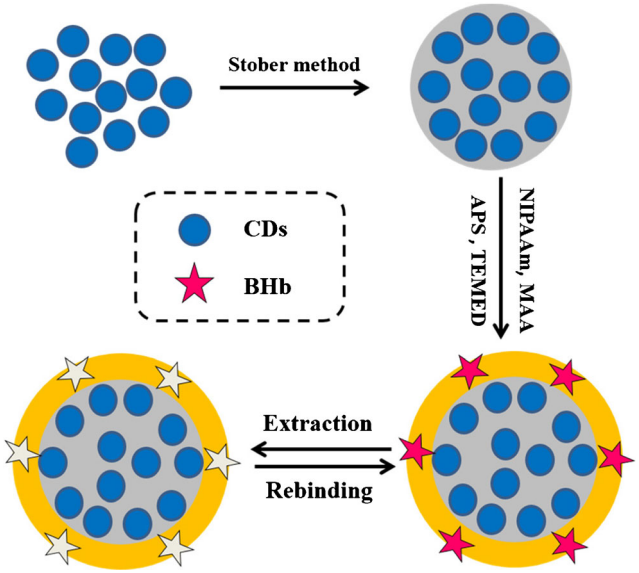

Fig. 1 Schematic illustration for the preparation procedure of CD@SiO_2@MIP

Results and discussion

Preparation and characterization of CD@SiO_2@MIP

Figure 1 represents the preparation process of CD@SiO_2@MIP. First, CDs were synthesized using one-step hydrothermal method and doped into silica to obtain uniform silanized CD composite (CD@SiO_2). Optically transparent silica protects the fluorescence intensity of CDs and provides biocompatibility, dispersibility, and surface functionality to CD@SiO_2 particles [34]. Subsequently, using CD@SiO_2 as fluorescent signal, NIPAAm and MAA as functional monomers, BHb as template molecule, MBA, APS, and TEMED as pre-polymerization reagents, the CD@SiO_2@MIP material was prepared, where a thin MIP shell was produced to coat the CD@SiO_2 (see Fig. 1). After the template BHb molecules were removed, some molecularly imprinted sites consistent with BHb were left in the shell layer. When the CD@SiO_2@MIP was added to BHb solution, the CD@SiO_2@MIP particles would rapidly adsorb the template BHb molecules, leading to the fluorescence quenching of the CD@SiO_2@MIP, and thus achieving the recognition toward the target molecule BHb.

The morphology and size for CDs, CD@SiO_2, and CD@SiO_2@MIPs were studied using transmission electron microscopy. As shown in Fig. 2 a, the average diameter of CD particles was about 3.05 nm, which is consistent with that reported in the literature [31]. In addition, the CDs were also characterized by FT-IR, XPS, and XRD, and results are represented in Figs. S1 and S2 (see ESM), demonstrating successful preparation of the CDs. Figure 2 b shows that the structure of the CD@SiO_2 particles are spherical, with uniform size of about 365 nm which is much larger than CDs, because many CDs were coated with silica in a CD@SiO_2 particle. The CD@SiO_2@MIP particles also have a uniform size of about 405 nm (Fig. 2c). The thickness of thin MIP layer can be calculated to be about 20 nm, which is beneficial to the specific recognition of the target protein.

Thermo-sensitive properties of the CD@SiO_2/MIP

It is well known that thermo-sensitive polymers reversibly swell and shrink with change in temperature. At a lower critical solution temperature (LCST) of ~32 °C, NIPAAm will undergo a phase transition [35]. To verify the thermal-sensitivity of the CD@SiO_2@MIP, a temperature-response test was carried out, providing the adsorption amounts of the template protein BHb (Fig. 3a) and the fluorescent intensities of the CD@SiO_2@MIP at 28 °C and 44 °C (Fig. 3b). The recognition of the CD@SiO_2@MIP to BHb exhibits significant temperature-dependence, meaning that the CD@SiO_2@MIP may be used as the temperature switch to control the capture/release of BHb. As shown in Fig. 3 a, the adsorption amount of BHb by the CD@SiO_2@MIP at 28 °C is higher than at 44 °C. At higher temperatures, the CD@SiO_2@MIPs appear as hydrophobic pellets with a weaker fluorescent signal (Fig. 3b), which is not conducive to their returning into the imprinted cavity again, and thus the adsorption amount is smaller. At lower temperatures, the CD@SiO_2@MIPs are transformed into hydrophilic pellets and therefore the fluorescence signal becomes stronger. Under this condition, it is more favorable for BHb to be recombined to the imprinted cavity, thus leading to a larger adsorption amount [15].

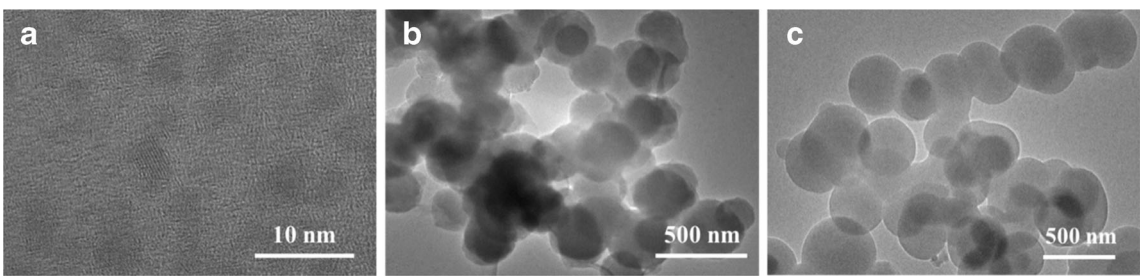

Fig. 2 Transmission electron microscopy images for **a** CDs, **b** CD@SiO_2, and **c** CD@SiO_2@MIP

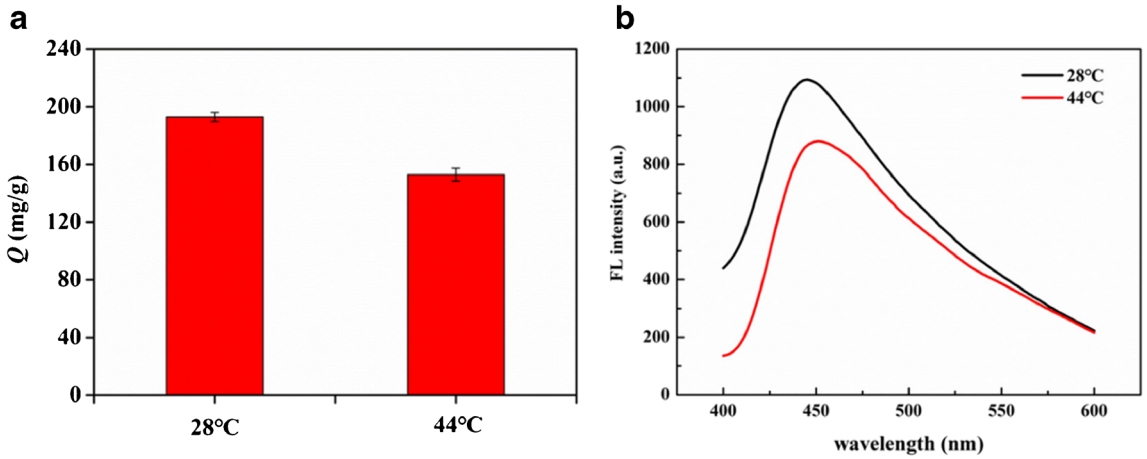

Fig. 3 Effect of temperature on **a** adsorption amount of the target protein BHb (Q) and **b** fluorescence intensities of CD@SiO_2@MIP. The error bar is based on three parallel experiments

Optical sensing property of the CD@SiO_2@MIP

To investigate the binding affinity property of CD@SiO_2@MIP and CD@SiO_2@NIP to the template BHb, their fluorescence tests were performed at different concentrations of BHb. Using the prepared CD@SiO_2@MIP, the purpose of identifying BHb was achieved by the fluorescence quenching due to the special interactions of the template molecules with the imprinting cavities. The fluorescence quenching follows the Stern-Volmer equation [36]:

$$F_0/F = 1 + K_{SV}c \quad (2)$$

where F_0 and F stand respectively for the fluorescent intensities of CD@SiO_2@MIP without and with BHb, K_{SV} is the Stern-Volmer constant, and c is the molarity of BHb.

The fluorescence spectra of the CD@SiO_2@MIP and CD@SiO_2@NIP for various molarities of BHb are shown in Figs. 4 a and b, respectively. Figure 4 shows that the fluorescent intensities of the CD@SiO_2@MIP and CD@SiO_2@NIP decrease linearly with increase in the BHb molarity. At the same molarity of BHb, the fluorescent intensity of CD@SiO_2@MIP exhibited a more decrease than that of CD@SiO_2@NIP. This is because some specific molecular recognition sites formed on the surface of CD@SiO_2@MIP are in accordance with size and shape of the template protein BHb molecule. Therefore, compared with non-molecularly imprinted polymers, molecularly imprinted polymers can adsorb more BHb molecules, resulting in a greater degree of fluorescence quenching.

The insets in Fig. 4 a and b show the BHb fluorescent quenching behavior for CD@SiO_2@MIP and CD@SiO_2@NIP, respectively. In a BHb concentration range (0.31–15.5 μM), the fluorescence quenching of the CD@SiO_2@MIP follows the equation: $F_0/F = 0.9178 + 7.0222\ c$ ($R^2 = 0.9952$), with a detection limit of 0.155 μM. Similarly, the fluorescence quenching behavior of the CD@SiO_2@NIP follows the equation: $F_0/F = 0.9454 + 2.2988\ c$ ($R^2 = 0.9940$). Consequently, the imprinting factor

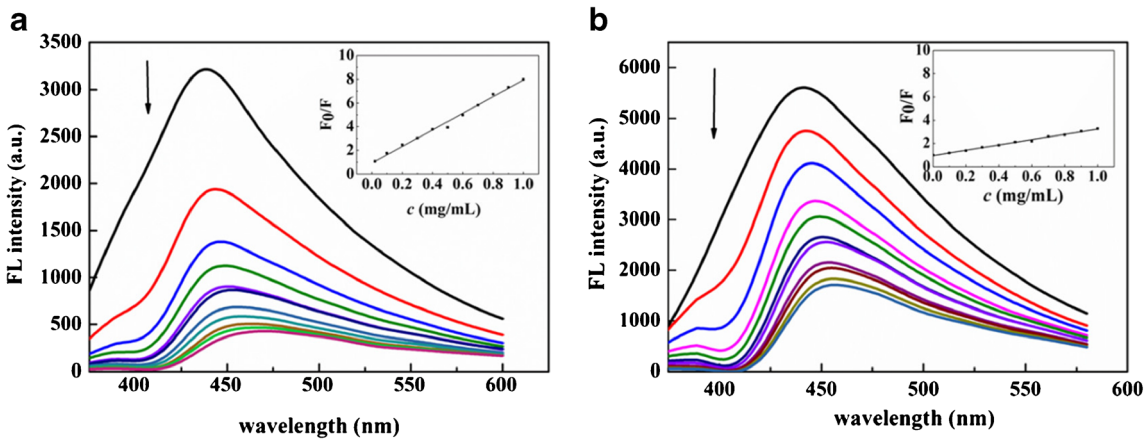

Fig. 4 Fluorescence emission spectra of **a** CD@SiO_2@MIP and **b** CD@SiO_2@NIP in different BHb concentration of 0 to 1.0 mg/mL. Insets in these two figures represent the Stern-Volmer plot. F_0 and F are the fluorescence intensity without and with BHb. Experimental conditions: concentrations of CD@SiO_2@MIP or CD@SiO_2@NIP are 1 mg/mL (PBS, 0.01 M, pH = 6.8), 28 °C, and $\lambda_{ex} = 345$ nm

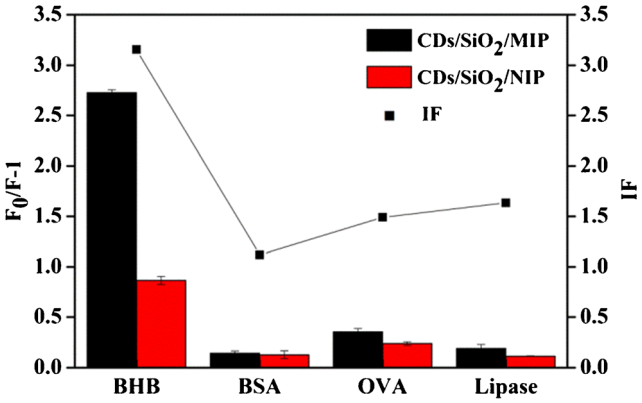

Fig. 5 Selectivity of CD@SiO_2@MIP and CD@SiO_2@NIP to some proteins and the imprinting factor (*IF*) of CD@SiO_2@MIP. F_0 and F are the fluorescence intensity without and with proteins: concentration of proteins is 1.2 mg/mL and $\lambda_{ex} = 345$ nm

($IF = K_{SV,MIP}/K_{SV,NIP}$, assessing the imprinting effect of CD@SiO_2@MIP as a sensor) was calculated to be 3.11. This indicates that the CD@SiO_2@MIP was good fluorescent sensor to quantitatively detect BHb.

Selective and competitive binding

To further demonstrate the selectivity of CD@SiO_2@MIP to BHb, other proteins like bovine serum albumin (BSA), ovalbumin (OVA), and lipase were selected as references. Figure 5 shows that the CD@SiO_2@MIP has the strongest fluorescent response to the template protein BHb. Compared with other proteins, BHb exhibited the largest fluorescence quenching ability to CD@SiO_2@MIP. The results confirm that as-prepared CD@SiO_2@MIP has a selective recognition ability to BHb. And this further proves that the cavity that is complementary to the templating molecule in morphology, size, and function-group was formed on the surface of the MIP shell during the preparation of CD@SiO_2@MIP. Thereby, the purpose of the selective capture of the target protein has been achieved. As for reference proteins, they are similar to BHb in sizes and structures, but not complementary to the recognition sites imprinted on the MIP. Therefore, these reference proteins cannot effectively quench the fluorescence of the CDs embedded in silica. The *IF* of CD@SiO_2@MIP for BHb is much larger than those for other proteins (see Fig. 5), indicating that the prepared CD@SiO_2@MIP has excellent selectivity to BHb. In addition, the selectivity of CD@SiO_2@MIP sensor was also confirmed by adsorption kinetic experiments (see ESM Fig. S3).

Figure 6 shows that the fluorescent intensity of CD@SiO_2@MIP hardly changes when the concentration ratio of the competitive proteins to BHb increases. Because the structure of competitive proteins does not match the specific sites imprinted by BHb, they cannot effectively quench the fluorescence of CD@SiO_2@MIP. These competition binding tests also confirm that CD@SiO_2@MIP has a good specific recognition ability to BHb. In addition, the results of recycling tests also indicate that CD@SiO_2@MIP has fine cyclic stability (ESM Fig. S4).

Table 1 Results for determination of BHb in the 100-fold diluted urine sample ($n = 3$)

Sample	Added (μM)	Found (μM)	Recovery ± RSD (%)
Urine	0.5	0.502 ± 0.013	100.4 ± 2.6
	1.0	0.986 ± 0.026	98.6 ± 2.6
	1.5	1.508 ± 0.013	100.5 ± 0.9

Analysis and detection of BHb in real sample

The practical applicability of the molecularly imprinted fluorescence sensors to BHb was further investigated in urine sample. It can be clearly seen from Table 1 that using the CD@SiO_2@MIP sensor, the recoveries of BHb in a 100-fold diluted urine sample ranged from 98.6 to 100.5%, with relative standard deviations (RSDs) of 0.85–2.6%. These results show that the sensor can determine sensitively and accurately the content of BHb in biological samples. Moreover, a comparison of our sensor is made with other MIP-based materials reported in the literature [37–41] (see Table 2), exhibiting that

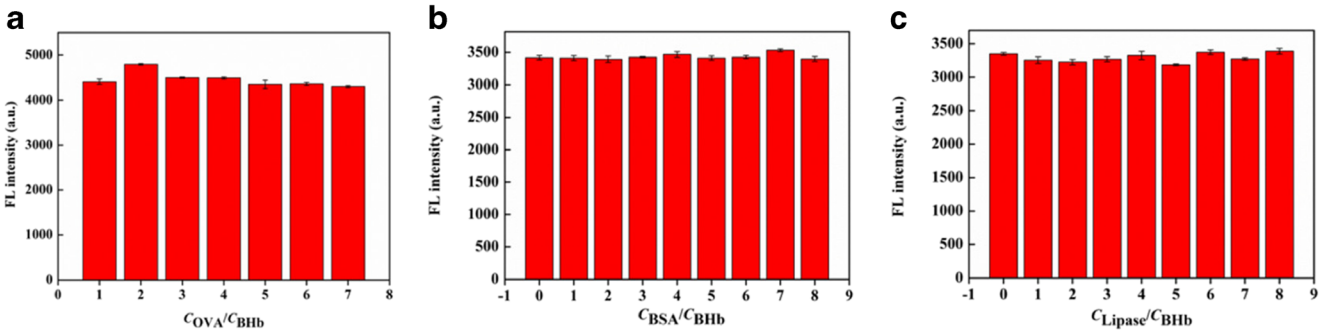

Fig. 6 Competition binding of CD@SiO_2@MIP with BHb and some competitive proteins at various ratios of BHb to competition proteins at 0.03 mg/mL of BHb (PBS = 0.01 M, pH = 6.8), at 28 °C, and $\lambda_{ex} = 345$ nm

Table 2 Comparison of analytical performance of the CD@SiO_2@MIP sensor with MIP-based fluorescence sensors previously reported for BHb detection

Material	Linear range (μM)	Detection limit (μM)	Sample	Recovery (%)	Ref
UCNPs/MOFs/MIP	1.6–9.3	0.961	–	–	[37]
CdTe/thermo-sensitive MIPs	0.28–4	0.16	Urine	98–110	[38]
BHb CdTe/MIPs	0.3–5.0	0.069	Bovine urine	97.0–103.0	[39]
M-CDs@MIPs	0.05–16.0	0.0173	Urine	102.0–102.7	[40]
Mn-doped ZnS QDs/MIP	0.1–5	0.038	Urine	96.7–103.8	[41]
CD/SiO_2/MIP	0.31–15.5	0.155	Urine	98.6–100.5	This work

our sensor possesses a comparable linear detection range and detection limit.

Conclusions

In summary, we successfully constructed a novel thermo-sensitive molecularly imprinted fluorescence sensor (CD@SiO_2@MIP) by using CDs as fluorescent signal and NIPAAm as thermo-sensitive monomer to detect BHb. The CD@SiO_2@MIP demonstrated good thermo-sensitive property and could be employed as a temperature switch to control the capture/release of the template molecule BHb. The sensor exhibited high selectivity and recognition specificity to the target protein BHb. Moreover, the sensor can accurately determine the content of BHb in real urine sample with recoveries of 98.6–100.5%. Consequently, the CD@SiO_2@MIP is expected to serve as a promising sensor material for special recognition and detection of BHb, and this strategy can also be expended to the detection of other proteins in biological fluids.

Funding information This study received financial supports from the National Natural Science Foundation of China (Nos. 21873026, 21573058, 21773059, 21303044).

Compliance with ethical standards

The informed consent was obtained from the healthy volunteer who provide urine sample for this study. All experiments in this study were approved by the Academic Ethics Committee of Henan Normal University, China, and have been performed in accordance with the ethical standards.

Competing interests The authors declare that they have no competing interests.

References

1. Duan L, He Q, Yan XH, Cui Y, Wang KW, Li JB. Hemoglobin protein hollow shells fabricated through covalent layer-by-layer technique. Biochem Biophys Res Commun. 2007;354:357–62.
2. Duan HM, Wang XJ, Wang YH, Li JB, Luo CN. Bioreceptor multi-walled carbon nanotubes@Fe_3O_4@SiO_2-surface molecular imprinted polymer in an ultrasensitive chemiluminescent biosensor for bovine hemoglobin. RSC Adv. 2015;5:88492–9.
3. Wang YQ, Zhang HM, Zhou QH. Studies on the interaction of caffeine with bovine hemoglobin. Eur J Med Chem. 2009;44:2100–5.
4. Chen LX, Xu SF, Li JH. Recent advances in molecular imprinting technology: current status, challenges and highlighted applications. Chem Soc Rev. 2011;40:2922–42.
5. Chen LX, Wang XY, Lu WH, Wu XQ, Li JH. Molecular imprinting: perspectives and applications. Chem Soc Rev. 2016;45:2137–211.
6. Wu Q, Li MN, Huang Z, Shao YM, Bai L, Zhou LC. Well-defined nanostructured core-shell magnetic surface imprinted polymers (Fe_3O_4@SiO_2@MIPs) for effective extraction of trace tetrabromobisphenol A from water. J Ind Eng Chem. 2018;60:268–78.
7. Gao DM, Zhang ZP, Wu MH, Xie CG, Guan GJ, Wang DP. A surface functional monomer-directing strategy for highly dense imprinting of TNT at surface of silica nanoparticles. J Am Chem Soc. 2007;129:7859–66.
8. Ge L, Wang SSM, Yu JH, Li NQ, Ge SG, Yan M. Molecularly imprinted polymer grafted porous Au-paper electrode for an microfluidic electro-analytical origami device. Adv Funct Mater. 2013;23:3115–23.
9. Ma Y, Pan PGQ, Zhang Y, Guo XZ, Zhang HQ. Narrowly dispersed hydrophilic molecularly imprinted polymer nanoparticles for efficient molecular recognition in real aqueous samples including river water, milk, and bovine serum. Angew Chem Int Ed. 2013;52:1511–4.
10. Xu SF, Lu HZ, Li JH, Song XL, Wang AX, Chen LX, et al. Dummy molecularly imprinted polymers-capped CdTe quantum dots for the fluorescent sensing of 2,4,6-trinitrotoluene. ACS Appl Mater Interfaces. 2013;5:8146–54.
11. Saylan Y, Yilmaz F, Ozgur E, Derazshamshir A, Yavuz H, Denizli A. Molecular imprinting of macromolecules for sensor applications. Sensors. 2017;17:898–928.
12. Li DY, He XW, Chen Y, Li WY, Zhang YK. Novel hybrid structure silica/CdTe/molecularly imprinted polymer: synthesis, specific recognition, and quantitative fluorescence detection of bovine hemoglobin. ACS Appl Mater Interfaces. 2013;5:12609–16.
13. Wang XY, Yu SM, Liu W, Fu LW, Wang YQ, Li JH, et al. A molecular imprinting based hybrid ratiometric fluorescence sensor for the visual determination of bovine hemoglobin. ACS Sens. 2018;3:378–85.
14. Yang YQ, He XW, Wang YZ, Li WY, Zhang YK. Epitope imprinted polymer coating CdTe quantum dots for specific

recognition and direct fluorescent quantification of the target protein bovine serum albumin. Biosens Bioelectron. 2014;54:266–72.
15. Li DY, Zhang XM, Yan YJ, He XW, Li WY, Zhang YK. Thermosensitive imprinted polymer embedded carbon dots using epitope approach. Biosens. Bioelectron. 2016;79:187–92.
16. Zhang Z, Li JH, Wang XY, Shen DZ, Chen LX. Quantum dots based mesoporous structured imprinting microspheres for the sensitive fluorescent detection of phycocyanin. ACS Appl Mater Interfaces. 2015;7:9118–27.
17. Li W, Sun Y, Yang CC, Yan XM, Guo H, Fu GQ. Fabrication of surface protein-imprinted nanoparticles using a metal chelating monomer via aqueous precipitation polymerization. ACS Appl Mater Interfaces. 2015;7:27188–96.
18. Bereli N, Andac M, Baydemir G, Say R, Galaev IY, Denizli A. Protein recognition via ion-coordinated molecularly imprinted supermacroporous cryogels. J Chromatogr A. 2008;1190:18–26.
19. Qin L, He XW, Zhang W, Li WY, Zhang YK. Macroporous thermosensitive imprinted hydrogel for recognition of protein by metal coordinate interaction. Anal Chem. 2009;81:7206–16.
20. Stobiecka M, Chalupa A. Modulation of plasmon-enhanced resonance energy transfer to gold nanoparticles by protein survivin channeled-shell gating. J Phys Chem B. 2015;119:13227–35.
21. Stobiecka M. Novel plasmonic field-enhanced nanoassay for trace detection of proteins. Biosens. Bioelectron. 2014;55:379–85.
22. Li H, Shao FQ, Zou SY, Yang QJ, Huang H, Feng JJ, et al. Microwave-assisted synthesis of N,P-doped carbon dots for fluorescent cell imaging. Microchim. Acta. 2016;183:821–6.
23. Wang WP, Lu YC, Huang H, Feng JJ, Chen JR, Wang AJ. Facile synthesis of water-soluble and biocompatible fluorescent nitrogen-doped carbon dots for cell imaging. Analyst. 2014;139:1692–6.
24. Huang H, Lv JJ, Zhou DL, Bao N. One-pot green synthesis of nitrogen-doped carbon nanoparticles as fluorescent probes for mercury ions. RSC Adv. 2013;3:21691–6.
25. Baker SN, Baker GA. Luminescent carbon nanodots: emergent nanolights. Angew Chem Int Ed. 2010;49:6726–44.
26. Mao Y, Bao Y, Han DX, Li FH, Niu L. Efficient one-pot synthesis of molecularly imprinted silica nanospheres embedded carbon dots for fluorescent dopamine optosensing. Biosens Bioelectron. 2012;38:55–60.
27. Wang H, Yi JH, Velado D, Yu YY, Zhou SQ. Immobilization of carbon dots in molecularly imprinted microgels for optical sensing of glucose at physiological pH. ACS Appl. Mater. Interfaces. 2015;7:15735–45.
28. Zhou Y, Qu ZB, Zeng YB, Zhou TS, Shi GY. A novel composite of graphene quantum dots and molecularly imprinted polymer for fluorescent detection of paranitrophenol. Biosens Bioelectron. 2014;52:317–23.
29. Liu HC, Ding L, Chen LG, Chen YH, Zhou TY, Li HY, et al. A facile, green synthesis of biomass carbon dots coupled with molecularly imprinted polymers for highly selective detection of oxytetracycline. J Ind Eng Chem. 2019;69:455–63.
30. Fang MY, Zhuo KL, Chen YJ, Zhao YJ, Wang JJ. Fluorescent probe based on carbon dots/silica/molecularly imprinted polymer for lysozyme detection and cell imaging. Anal Bioanal Chem. 2019;411:5799–807.
31. Zhu SJ, Meng QN, Wang L, Zhang JH, Song YB, Jin H, et al. Highly photoluminescent carbon dots for multicolor patterning, sensors, and bioimaging. Angew Chem Int Ed. 2013;52:3953–7.
32. Stöber W, Fink A. Controlled growth of monodisperse silica spheres in the micron size range. J Colloid Interface Sci. 1968;26:62–9.
33. Zhang X, Yang S, Sun LQ, Luo AQ. Surface-imprinted polymer coating L-cysteine-capped ZnS quantum dots for target protein specific recognition. J Mater Sci. 2016;51:6075–85.
34. Yang YH, Gao MY. Preparation of fluorescent SiO_2 particles with single CdTe nanocrystal cores by the reverse microemulsion method. Adv Mater. 2005;17:2354–7.
35. Lutz JF, Akdemir O, Hoth A. Point by point comparison of two thermosensitive polymers exhibiting a similar LCST: is the age of poly (NIPAM) over. J Am Chem Soc. 2006;128:13046–7.
36. Chen YF, Rosenzweig Z. Luminescent CdS quantum dots as selective ion probes. Anal Chem. 2002;74:5132–8.
37. Guo T, Deng QL, Fang GZ, Gu DH, Yang YK, Wang S. Upconversion fluorescence metal-organic frameworks thermosensitive imprinted polymer for enrichment and sensing protein. Biosens Bioelectron. 2016;79:341–6.
38. Zhang W, He XW, Li WY, Zhang YK. Thermo-sensitive imprinted polymer coating CdTe quantum dots for target protein specific recognition. Chem Commun. 2012;48:1757–9.
39. Wang XY, Yu JL, Li JH, Kang Q, Shen DZ, Chen LX. Quantum dots based imprinting fluorescent nanosensor for the selective and sensitive detection of phycocyanin: a general imprinting strategy toward proteins. Sens Actuat B-Chem. 2018;255:268–74.
40. Lv PP, Xie DD, Zhang ZH. Magnetic carbon dots based molecularly imprinted polymers for fluorescent detection of bovine hemoglobin. Talanta. 2018;188:145–51.
41. Tan L, Kang CC, Xu SY, Tang YW. Selective room temperature phosphorescence sensing of target protein using Mn-doped ZnS QDs-embedded molecularly imprinted polymer. Biosens. Bioelectron. 2013;48:216–23.